Stability, electronic and defect levels induced by substitution of Al and P pair in 4H–SiC

E. Igumbor[a,*], G.M. Dongho-Nguimdo[a], R.E. Mapasha[b], E. Omotosoc, W.E. Meyer[b,**]

[a] College of Science, Engineering and Technology, University of South Africa, P.O.Box 392 UNISA, 0003, Pretoria, South Africa

[b] Department of Physics, University of Pretoria, Pretoria, 0002, South Africa

[c] Department of Physics and Engineering Physics, Obafemi Awolowo University, Ile-Ife, Nigeria

* Corresponding author.
** Corresponding author.
E-mail addresses: elgumuk@gmail.com (E. Igumbor), wmeyer@up.ac.za (W.E. Meyer).

Highlights

- The double substitution of P and Al in 4H–SiC occurs with relatively low energy and stable with respect to their binding energies.
- The substitution of P/Al on Si sites is under equilibrium conditions, more energetically favourable than other defects.
- Defect levels were induced by the P and Al substitutional pair in 4H–SiC.
- All the acceptor levels induced in the band gap of 4H–SiC are always shallow and close to the conduction band minimum.
- The results of this report will provide more frontier insight for the synthesis of the substitution of P and Al pair in 4H–SiC.

Abstract

Impurities play a major role in identifying the most enhanced defect-levels induced in 4H−SiC. Among the important *n*- and *p*-type dopants in SiC are the P and Al, respectively. The P and Al dopants modify the 4H−SiC electronic structure and induce notable defect-levels which may influence the host's performance. In this report, the Heyd, Scuseria and Ernzerhof hybrid functional was used to predict the energetic, stability, electronic properties and defect levels induced by P and Al substitutional pair in 4H−SiC. The $P_{Si}Al_{Si}$ configurations of the P and Al substitutional pair in 4H−SiC in its neutral charge state, under equilibrium conditions, is more energetically favourable with a formation energy of 0.21 eV. The substitution of P and Al pair in 4H−SiC for the different configurations are energetically stable with respect to their binding energies. The $P_{Si}Al_C$ configuration with respect to its binding energy shown low tendency to dissociate into a non-interacting defects with an energy of 4.00 eV compared to other defects. Defect levels were induced by the P and Al substitutional pair in 4H−SiC. A deep (+2/+1) level and shallow (+1/0) and (0/−1) levels were predicted for the P_CAl_C and P_CAl_{Si}. In all defect configurations, the (0/−1) defect level was found to be close to the conduction band minimum. The results of this report provide frontier insight for the synthesis of the substitution of P and Al pair in 4H−SiC.

Keywords

Defect; Formation energy; Charge state; Substitution pair

1. Introduction

Among the wide band gap semiconductor materials generating interest for high energy and high frequency applications, silicon carbide (SiC) is outstanding. Due to the recent developments in crystal growth, high quality polytypes of SiC have become available, hence, creating a renewed interest. SiC can operate at high temperature and high frequency which makes it suitable for producing high frequency electronic devices [1,2]. SiC radiation hardness allows its operation as a material in nuclear reactors and with further application in radiation harsh environments (space, accelerator facilities and nuclear power plants) [1,3,4]. In the number of the SiC polytypes, the 4H−SiC is known to be the most promising polytype for high temperature and high power device applications owing to its larger band gap and a higher isotropic electron mobility compare to others [5]. The 4H−SiC has an experimental band gap of 3.26 eV [2,[6], [7], [8]], which is

larger than any other polytype band gap. As a result, it is expected that defect thermodynamic charge state transition levels will occur well in the band gap compare to other polytypes. Defects have been known to influence the performance of semiconductor materials [6,9,10]. As an example, the doping of 4H–SiC with transition metals influences its electronic and thermal properties [11]. This in some cases may lead to performance degradation when exposed to irradiation. Based on the knowledge that the realisation of SiC based applications demands high crystalline quality, it is important to know the extent at which defects can influence it. The substitutional doping of SiC is usually performed by ion-implantation, whereby damages to the crystal may occur depending on the level of fluence and type of ions used. Upon damage, some of the crystal atoms are displaced from their lattice sites causing large concentration of vacancies and interstitials [12,13]. In order to control the level of damage, a subsequent annealing is employed at high temperature. This process allows the vacancies and interstitials to recombine and the dopant atoms are incorporated at the substitutional sites. Techniques such as chemical vapour deposition (CVD) and molecular beam epitaxy (MBE) have been successfully used to grow and fabricate high purity SiC [[14], [15], [16]]. Another promising alternative technique used to grown SiC is ion beam synthesis (IBS), where high-dose C is implanted at high temperatures into Si and further annealed to form SiC layers [17,18]. Earlier study revealed that implanted carbon suppresses transient enhanced diffusion of B or P dopant in SiC during annealing [19]. This is most often exploited to create a shallow *p-n* junctions in sub-micron technologies. Because of its high breakdown field, 4H–SiC is well suited for high voltage switching device with potential applications in motor control, electric power conditioning and distribution. As a result, several efforts have been put in place to realised a high voltage Schottky

barrier *p-n* junctions. However, the electrical performance of some devices is degraded with continuous switching which is associated to the formation of triangular defects. Diverse point defects in 4H–SiC have been reported to play important roles in enhancing the activities of the defect concentrations as well as defect levels induced in the band gap [3,[20], [21], [22], [23]]. Studies related to the understanding of defects via experiment methods have previously been carried out [[24], [25], [26], [27]]. For example, electron irradiation result of the substitution of Al atom in SiC shows that the density of the defective system is reduced by 4.6 MeV [28,29]. Furthermore, the ion-implantation of P in 4H–SiC is adjudicated to be responsible for the high density interface which further increases the peak field-effect-mobility of 4H–SiC metal-oxide semiconductor field-effect-transistors [20,21,30]. Hence, as a result of the elimination of the Si–

Si bonds, the P atom in 4H–SiC might lead to the passivation of near-interface traps. This P passivation in 4H–SiC removes states from the conduction band of its host [20,30]. The radiation damage of Al related defects in SiC have been reported [[31], [32], [33], [34]]. Reports have shown that during irradiation of Al-doped SiC, the Al atom forms thermal stable complex with two C_iC_i (C_i is C interstitial), carbon vacancy V_C, as well as metastable complexes with C_i or C_iC_i and induce deep level defects in the band gap of SiC [28]. Double substitutional defect such as C_sC_s (C_s is carbon substitution) is suggested to produces interfacial states in and around the band gap of SiC [35]. According to electron paramagnetic resonance report, the Al substitution is a shallow defect on the Si site in SiC [28,36] which induced E_V+0.82 and E_V+1.01 eV (E_V is the energy of the valence band maximum) defect levels. Some hole traps in a p-type and electron trap in a n-type 4H–SiC epitaxial films have been reported [37]. For the n-type doping, the N and P atoms are most often used as dopants for low sheet resistance as well as a deep range implantation. The Al atom on the other hand, is commonly used as a p-type dopant. Kawahara et al. investigated deep levels in the whole energy range of band gap of 4H–SiC, which are generated by low-dose N^+, P^+, and Al^+ n-type and p-type implantation, respectively, using the deep level transient spectroscopy (DLTS) [38]. Their study showed that the pair of Al^+/B^+ and N^+/P^+ implanted in SiC induced deep defect levels at the valence band maximum (VBM) and conduction band minimum (CBM), respectively. In spite of the physical behaviour of Al^+/B^+, N^+/P^+ p/n-type defects in 4H–SiC and their defect levels, there are no current detailed reports of the theoretical predictions of co-implantation of the P and Al substitutional pair in 4H–SiC, hence the motivation for this study. The first hand knowledge of the theoretical prediction of the electronic and defect levels induced by the co-implantation of the P and Al pair in 4H–SiC could create an interesting avenue for the synthesis of n/p-type related device for defects engineering and control.

In order to provide more insight to the defect levels induced in 4H–SiC that may arise as a result of the co-implantation of the P and Al pair, we have carried out a hybrid density functional theory calculations using the Heyd, Scuseria and Ernzerhof (HSE06) [39]. The substitution of P and Al pair in various lattice sites of Si or C atoms of 4H–SiC forming different substitutional-complex configurations were explored. The formation energy and the stability of these substitutional-complexes were predicted including the role of the defect levels induced in them. Our results shown that the various configurations of the substitutional-complexes of P and Al pair in 4H–SiC were stable with respect to

their binding energies and dissociation could only be feasible at the expense of energy higher than the formation energy. In addition, while the P_CAl_C and $P_{Si}Al_C$ induced double donor levels, the $P_{Si}Al_{Si}$ and P_CAl_{Si} induced single donor and acceptor levels. All the acceptor levels induced in the band gap of 4H–SiC were shallow and close to the CBM.

2. Computational details

Density function theory (DFT) modelling of the electronic and charge state transition levels of P and Al substitution pair in 4H–SiC was performed using the Vienna *ab-initio* Simulation Package (VASP) [40]. In the VASP code, the DFT calculation uses the chemically active valence electron, as the core electrons are always frozen. To separate the core from the valence electrons, the projector-augmented wave (PAW) method [41] was used. While the $2s^2$ and $2p^2$ valence electrons of C and the $3s^2$, $3p^2$ valence electrons of Si were included in our calculations, for P and Al, the $3s^2$, $3p^3$ and $3s^2$, $3p^1$ were respectively used as the valence electrons. All calculations were performed using the HSE06 hybrid functional with the Perdew, Burke and Ernzerhof (PBE) [42]. In the HSE06 approach, the PBE is mixed with the non-local Fock. For the calculations presented in this report, a mixing parameter of 0.25 of the HSE06 was used to predict a band gap of 3.23 eV, which is close to the experimental band gap of 3.26 eV at 300 K as reported by Levinshtein et al. [43] as well as other theoretical band gap predictions [[44], [45], [46]]. For us to model defects in 4H–SiC using the supercell approach, we constructed a supercell from a relaxed primitive unit cell of 4H–SiC. The predicted lattice parameters of 3.07 Å, 10.05 Å and 3.27, for the *a*, *c* and c/a, respectively of the relaxed unit cell 4H–SiC (which belongs to the space group P_{63mc}), are in agreement with earlier reports [43,45,46]. A well converged supercell as documented in Ref. [44], containing 96 atoms as shown in Fig. 1a was adopted for this study. Based on this well converged 96 atoms supercell of the 4H–SiC, we introduced the P and Al atoms either on the C or Si atom site, or on both C and Si atomic sites. The following configurations $P_{Si}Al_C$ (as displayed in Fig. 1b), P_CAl_C, $P_{Si}Al_{Si}$ and P_CAl_{Si} (see Fig. 1c) were considered. The relaxed structural properties of the 4H–SiC with Al and P defects are already reported in Ref. [45]. The supercell containing the defects was held fixed and all atoms were relaxed until the forces acting on them were less than 0.01 eV/Å. This was

achieved with a convergence criteria of 400 eV for the energy cut-off and a total energy difference lower than 10^{-5} eV. The well converged energy cut-off of 400 eV has been previously used to modelled the electronic and defect properties of SiC

[[47], [48], [49], [50]], and it was sufficiently used to reproduced the lattice parameters and band gap of the 4H−SiC in this study. The Brillouin zone was integrated with a Monkhost-Pack special k-points mesh of $2 \times 2 \times 2$. For the density of states calculations, a denser $8 \times 8 \times 8$ k-points mesh was used. The formation energy = $E^F\left(substituion - pair, q\right)$ of the substitution of P and Al pair in 4H−SiC for its charge state q as a function of the electron Fermi energy (ε_F) is given as

$$E^F\left(substituion - pair, q\right) = E\left(substituion - pair, q\right) - E\left(4H - SiC\right) + \sum_i \triangle(n)_i \mu_i, + q\left[E_V + \varepsilon_F\right] + E^q_{FNV}. \quad (1)$$

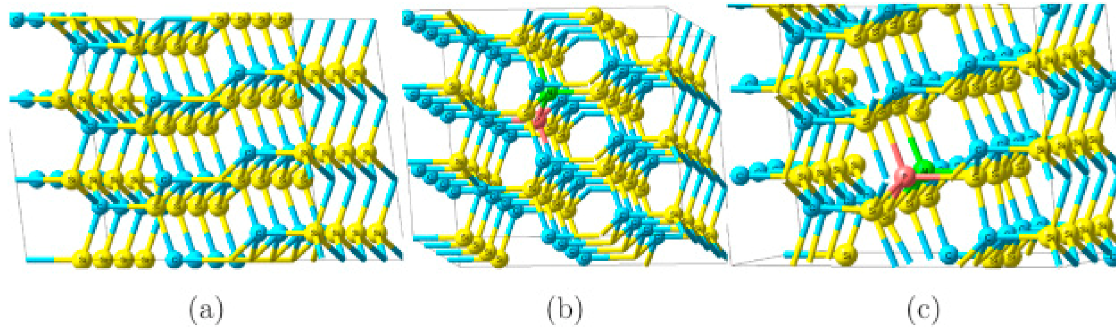

Fig. 1. The relaxed geometric structures of the (a) pristine supercell of 4H−SiC containing 96 atoms; (b) $P_{Si}Al_C$ (P and Al substituted for Si and C, respectively) and (c) $P_{Si}Al_{Si}$ (P and Al substituted for Si).

The total energy of the P and Al substitutional pair, total energy of the pristine supercell of 4H−SiC, the number of removed or added constituent atoms of type ith and the energy of the valence band maximum (VBM) are represented by $E\left(substituion - pair, q\right)$, $E\left(4H - SiC\right)$, $\triangle(n)_i$ and E_V, respectively. The correction term E^q_{FNV} according to the method of Ref [51], was included to account for the errors that may arise as a result of finite-size effect and defect-defect interactions. The μ_i is the chemical potential of the type ith constituent atom. The criteria for calculating the chemical potentials of the C and Si atoms and their values where taken from Ref. [52]. While the μ_P was calculated using the total energy of P body centred cubic (BCC) structure, μ_{Al} was calculated using the a face centred structure (as the total energy per number of Al atom) as previously reported in Ref. [45].

3. Results and discussion

Different atom lattice sites of Si and C atoms were considered for impurity substitutions. This includes two major impurity positions; (i) when the impurity atoms were nearest neighbour and (ii) when the impurity atoms were far apart (not nearest neighbour). The formation energy of all defect configurations with respect to impurities positions considered in this study shown to be more stable when impurity atoms are nearest neighbour. In this work, the nearest neighbour (as shown in Fig. 1b and c) results of all the defect configurations of P–Al pair substitution in 4H–SiC were reported.

3.1. Electronic properties

Fig. 2 displays plots of the total density of states (TDOS) on the left panel and the partial density of states (PDOS) on the right panel. According to Fig. 2a–d, the presence of defects in 4H–SiC induced ground state orbitals that populated the gap close to the valence band maximum (VBM) around the Fermi level. For the P_CAl_C, sharp peaks were introduced around the VBM (see Fig. 2a). These peaks were contributed by the ground state $3p$-orbital of the Si, Al and P atoms. Strong orbital hybridization between the p orbital of the Si, Al and P atoms was also observed. Whereas the P_CAl_{Si} and $P_{Si}Al_{Si}$ have almost the same shape of the PDOS as displayed by Fig. 2b and c, respectively, the P_CAl_C and $P_{Si}Al_C$ have same peculiar behaviour. For example, the P_CAl_C and $P_{Si}Al_C$ populated ground state orbitals around the Fermi level have strong sharp peaks. According to Fig. 2d, the presence of defects for the case of $P_{Si}Al_C$ introduced orbital ground state with sharp peaks lying below the Fermi level (which are consequence of $3p$-orbital of the Al and P atoms) in the band gap of the host. The $3p$-orbital of the Si atom hybridizes with the $3p$-orbital of the P as well as the Al atom. In general, from the plots of the PDOS it was observed that the substitution of P and Al pair in 4H–SiC acts as a *p*-type material. We further noticed that the P_CAl_C, $P_{Si}Al_C$, $P_{Si}Al_{Si}$ and P_CAl_{Si} did not alter the spin orientation of the pristine 4H–SiC, hence, no evidence of spin polarisation was observed. This further shows that the host and participating atoms are non-magnetic, and introduction of P and Al defects does not induced magnetic moment in 4H–SiC.

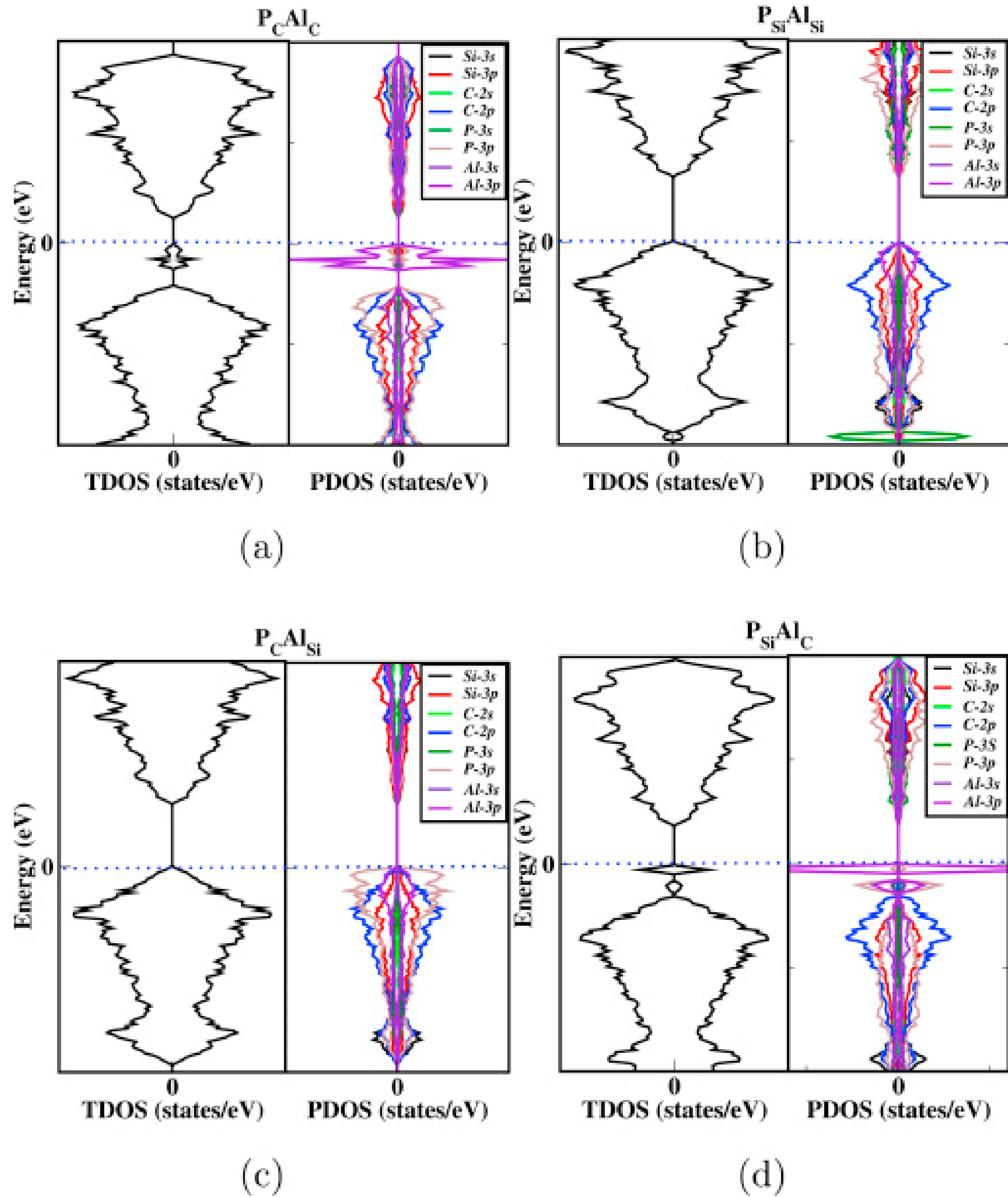

Fig. 2. Plots of the total density of states TDOS, left panel and partial density of states, PDOS, right panel for the (a) P_CAl_C; (b) $P_{Si}Al_{Si}$; (c) P_CAl_{Si} and (d) $P_{Si}Al_C$. The horizontal dash line is the ε_F, which is set to zero.

3.2. Formation and stability of defects

Table 1 displays the formation and binding energies of the P_CAl_C, $P_{Si}Al_C$, $P_{Si}Al_{Si}$ and P_CAl_{Si} in their zero charge state. The formation energy shown that the substitution of both P and Al pair in 4H−SiC at Si lattice sites is more energetically

favourable (with E^F = 0.21 eV). This highlights the preference of the Al and P impurity to the Si lattices compared to the C lattice sites. When P and Al were substituted for the nearest two C atoms, the corresponding defect had a relatively high formation energy of 18.93 eV. The P_CAl_{Si} and $P_{Si}Al_C$ have formation energies of 5.87 and 11.79 eV respectively. The high formation energy of the P_CAl_C is attributed to the relatively high formation energy of the P_C and Al_C compared to the P_{Si} and Al_{Si} as reported in literature [28,36].

Table 1. The energy of formation (E^F) and binding energy (E_B) in eV at ε_F = 0 for the P and Al substitution pair in 4H–SiC. The E^F and E_B energies were calculated under chemical potential rich conditions.

	P_CAl_C	$P_{Si}Al_{Si}$	P_CAl_{Si}	$P_{Si}Al_C$
E^F	18.93	0.21	5.87	11.79
E_B	2.35	3.14	2.97	4.00

In a double substitution defects, it is paramount to ascertain if the parent defect will dissociate into a smaller non-interacting defects (P_C, Al_C, P_{Si} or Al_{Si}). This was confirmed by evaluating the binding energy of the parent defect. The binding energy E_B of double substitution of P and Al on C sites (P_CAl_C) is defined as the energy required to split the P_CAl_C into a non-interacting P_C and Al_C. The binding energy is given as [53].

$$E_B = E^F_{P_C} + E^F_{Al_C} - E^F_{P_C Al_C} \tag{2}$$

where $E^F_{P_C}$, $E^F_{Al_C}$ and $E^F_{P_C Al_C}$ are the neutral charge state formation energies of the P_C, Al_C and P_CAl_C, respectively. This same definition of the binding energy is applicable to other double substitutional defects in this study. According to Eq. (2), if $E_B > 0$, this implies a stable double substitutional defect. However, if the $E_B < 0$, dissociation of the substitution of P and Al pair in 4H–SIC is imminent with an energy lower than the energy of formation. The binding energies of the P_CAl_C, $P_{Si}Al_{Si}$, P_CAl_{Si} and $P_{Si}Al_C$ as calculated using Eq. (2) were all positive. The implication is that the aforementioned defective systems, are stable and dissociation is unlikely to occur, except at the expense of a much higher energy. The most stable double substitutional defect was the $P_{Si}Al_C$ with binding energy of 4.00 eV. This same behaviour has been reported for the $N_{Si}B_C$ which has the highest binding energy for the substitution of N and B pair in 4H–SiC [44]. The

$P_{Si}Al_C$ will need an additional 4.00 eV or more energy to separate into non interacting P_{Si} and Al_C defects. Furthermore, a close look at the binding energies suggest that the P_CAl_C with the highest formation energy is stable with binding energy of 2.35 eV, which is 0.62 eV lower than the binding energy of the P_CAl_{Si}. Based on the results of the binding energy, we suggest that at a relatively low annealing temperature, these defects will not dissociate. However, as the temperature increases, the formation energy eventually increases surpassing the formation energies listed in Table 1. Consequently, the defect-complex could dissociates into a more stable system of non-interacting defects.

3.3. Charge state transition level

The defect charge state transition level ($\varepsilon\,(q/q')$) is the formation energy at which q and q' are the same and was calculated using the method of Refs [54] as

$$\varepsilon\,(q/q') = \frac{E^f(d,q;\varepsilon_F=0)-E^f(d,q';\varepsilon_F=0)}{q'-q}, \tag{3}$$

where $E^f\,(d,q;\varepsilon_F=0)$ is the formation energy of the defect d (substitution-pair) in charge state q at Fermi energy equals to zero. Table 2 lists the defect induced energy levels of the P and Al substitution pair in 4H−SiC. Fig. 3 displays the plot of formation energy as a function of the Fermi energy. For the P_CAl_C, we observed the presence of three distinct defect levels: ((+2/+1), (+1/0) and (0/−1)) as displayed by Fig. 3a. The donor defect levels were all lying deep in the band gap of 4H−SiC with energies of $E_V+0.55$ eV for the double donor (+2/+1) and $E_V+0.97$ eV for the single donor (+1/0). The (0/−1) acceptor defect level was shallow, close to the CBM with an energy level of $E_C-0.16$ eV. The $P_{Si}Al_{Si}$ on the other hand, induced two notable shallow defect levels (see Fig. 3b). The two defect levels are the (+1/0) donor and (0/−1) acceptor with energies of E + V0.08 and E−C0.09 eV, respectively. Reports suggest that the P_{Si} is a shallow donor whereas the Al_{Si} is a shallow acceptor [36,55]. These could be the possible reasons for the shallow donor and shallow acceptor levels induced by the $P_{Si}Al_{Si}$. The P_CAl_{Si} as displayed in Fig. 3c induced deep donor levels and shallow acceptor level. Whereas the E−C0.11 eV energy level of the (0/−1) acceptor is close to the CBM, the (+1/0) energy level is 0.15 eV far away from the VBM. The $P_{Si}Al_C$ on the other hand, induced defect levels, an acceptor and double donors. The (+2/+1) donor is a deep defect level with an energy of 0.32 eV far away from the VBM. The single donor and acceptor defect levels, (+1/0) and (0/−1) (see Fig. 3d) have energies of E + V0.57 and E−C0.05 eV, respectively. The E_V+0.97 eV of the P_CAl_C is within the range of the defect level of E_V+0.82 to E_V+1.01 induced by the Al implanted in SiC [23].

Table 2. The thermodynamic charge state transition ($\varepsilon\,(q/q')$) level above the VBM in eV as induced by the P and Al substitution pair in 4H–SiC.

Defect	$(+2/+1)$	$(+1/0)$	$(0/-1)$
P_CAl_C	0.55	0.97	3.07
$P_{Si}Al_{Si}$	–	0.08	3.14
P_CAl_{Si}	–	0.15	3.12
$P_{Si}Al_C$	0.32	0.57	3.18

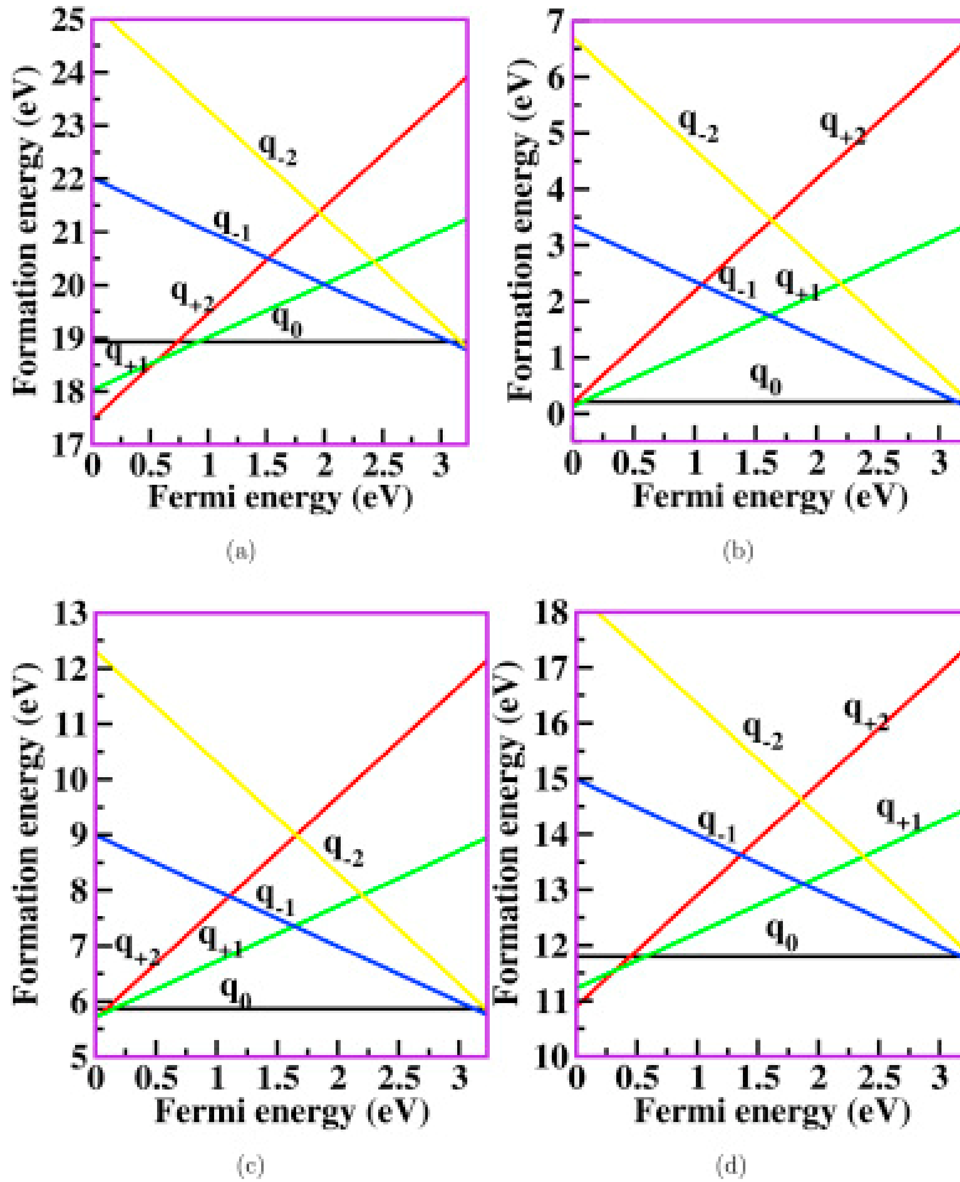

Fig. 3. Plots of formation energy as a function of the Fermi energy for the charge state (q_n; n = 0, ±1 ±2) of the substitution of P and Al pair in 4H–SiC; (a) P_CAl_C; (b) $P_{Si}Al_{Si}$; (c) P_CAl_{Si} and (d) $P_{Si}Al_C$.

More insight into the general trend of P and Al substitution pair in 4H−SiC was explored. While the defects with Al_C induced double donor levels, we observed that the defects formed with Al_{Si} induced shallow single donor and acceptor levels. This scenario shown that when the defects have excess Si than C atoms, the presence of double donor level is prevalent. However, when the defect has excess C atoms there is only a single shallow defect level induced. One interesting occurrence in this study was the absence of double acceptor level, instead the presence of single acceptor level is dominant in the band gap for all the defect studied. Whereas all induced acceptor levels were shallow and close to the CBM, the (0/−1) of the $P_{Si}Al_C$ was closer to the CBM relatively to other defect configurations. While the substitution of P and Al pair in 4H−SiC for all configurations induced single donor level, only the $P_{Si}Al_{Si}$ and P_CAl_{Si} induced shallow donor level close to the VBM.

4. Summary

This report employed the use of HSE06 to obtained the defect levels induced by substitution of P and Al pair in 4H−SiC. The formation energies of various unique defects considered showed that the Al and P atoms on the lattice sites of Si atom is more energetically stable under equilibrium conditions than when they are on the lattice sites of C atom. The binding energies of the defects revealed that they are stable and dissociation will only occur at the expense of energy higher than their formation energy. Under equilibrium conditions, we found that the most energetically favourable defect is the $P_{Si}Al_{Si}$ with an energy of formation of 0.21 eV. All the defects were observed to be electrically active. The $P_{Si}Al_{Si}$ and P_CAl_{Si} induced shallow defect levels close to the VBM and the CBM for the donor and acceptor, respectively. The P_CAl_C and $P_{Si}Al_C$ only induced deep single donor and acceptor levels. The information provided in this report will be beneficiary for the characterisation of SiC based devices for industrial and laboratory applications.

CRediT authorship contribution statement

E. Igumbor: Writing - original draft, Conceptualization, Methodology, Writing - review & editing. **G.M. Dongho-Nguimdo:** Writing - review & editing. **R.E. Mapasha:** Conceptualization, Methodology, Writing - review & editing. **E. Omotoso:** Writing - review & editing. **W.E. Meyer:** Supervision, Writing - review & editing, Funding acquisition.

Declaration of competing interest

The authors declare that they have no known competing financial interests or personal relationships that could have appeared to influence the work reported in this paper.

Acknowledgement

This work is based on the research supported partly by National Research foundation (NRF) of South Africa (Grant specific unique reference number (UID) 98961). The opinions, findings and conclusion expressed are those of the authors and the NRF accepts no liability whatsoever in this regard. EI and GMDN thank the University of South Africa (UNISA) for financial supports and the Center for High Performance Computing (CHPC) Cape Town for providing computational resources.

References

[1] Akira Itoh, Tsunenobu Kimoto, Hiroyuki Matsunami, *IEEE Electron. Device Lett*. 16 (6) (1995) 280–282.
[2] G.Y. Chung, C.C. Tin, J.R. Williams, K. McDonald, R.K. Chanana, Robert A. Weller, S.T. Pantelides, Leonard C. Feldman, O.W. Holland, M.K. Das, et al., *IEEE Electron. Device Lett*. 22 (4) (2001) 176–178.
[3] E. Omotoso, W.E. Meyer, P.J. Janse van Rensburg, E. Igumbor, S.M. Tunhuma, P.N. M. Ngoepe, H.T. Danga, F.D. Auret, *Nucl. Instrum. Methods Phys. Res. Sect. B Beam Interact. Mater. Atoms* 409 (2017) 241–245.
[4] J. Cottom, G. Gruber, P. Hadley, M. Koch, G. Pobegen, T. Aichinger, A. Shluger, *J. Appl. Phys*. 119 (18) (2016), 181507.
[5] C. Codreanu, M. Avram, E. Carbunescu, E. Iliescu, *Mater. Sci. Semicond. Process.* 3 (1–2) (2000) 137–142.
[6] Shi-Yi Zhuo, Xue-Chao Liu, Wei Huang, Ting-Xiang Xu, Wei-Wei Han, Cheng-Feng Yan, Er-Wei Shi, *AIP Adv*. 8 (12) (2018), 125001.
[7] V.E. Gora, F.D. Auret, H.T. Danga, S.M. Tunhuma, C. Nyamhere, E. Igumbor, A. Chawanda, *Mater. Sci. Eng., B* 247 (2019), 114370.
[8] E. Omotoso, F.D. Auret, E. Igumbor, S.M. Tunhuma, H.T. Danga, P.N.M. Ngoepe, B. A. Taleatu, W.E. Meyer, *Appl. Phys. A* 124 (5) (2018) 395.
[9] Emmanuel Igumbor, Richard Charles Andrew, Walter Ernst Meyer, *J. Electron. Mater*. 46 (2) (2017) 1022–1029.
[10] Emmanuel Igumbor, Ezekiel Omotoso, Helga T. Danga, Shandirai Malven Tunhuma, Walter Ernst Meyer, *Nucl. Instrum. Methods Phys. Res. Sect. B Beam Interact. Mater. Atoms* 409 (2017) 9–13.

[11] Norbert Achtziger, Wolfgang Witthuhn, *Appl. Phys. Lett*. 71 (1) (1997) 110–112.
[12] Brendan Campbell, Wahid Choudhury, Alison Mainwood, Mark Newton, Gordon Davies, Lattice damage caused by the irradiation of diamond, *Nucl. Instrum. Methods Phys. Res. Sect. A Accel. Spectrom. Detect. Assoc. Equip*. 476 (3) (2002) 680–685.
[13] Miaomiao Yuan, Xia Zhang, MA Saeedi Ahmad, Wei Cheng, Chungang Guo, Bin Liao, Xu Zhang, Minju Ying, Gillian A. Gehring, Study of the radiation damage caused by ion implantation in zno and its relation to magnetism, *Nucl. Instrum. Methods Phys. Res. Sect. B Beam Interact. Mater. Atoms* 455 (7–12) (2019).
[14] K. Mochizuki, S. Ji, R. Kosugi, Y. Yonezawa, H. Okumura, in: Electron *Devices Meeting (IEDM), 2017 IEEE International*, vols. 35–4, 2017. IEEE.
[15] D.J. Larkin, *Phys. Status Solidi* 202 (1) (1997) 305–320.
[16] F La Via, A. Severino, R. Anzalone, C. Bongiorno, G. Litrico, M. Mauceri, M. Schoeler, P. Schuh, P. Wellmann, *Mater. Sci. Semicond. Process*. 78 (2018) 57–68.
[17] Akiyoshi Chayahara, Masato Kiuchi, Atsushi Kinomura, Yoshiaki Mokuno, Yuji Horino, Kanenaga Fujii, Jpn. *J. Appl. Phys.* 32 (9A) (1993) L1286.
[18] K Kh Nussupov, N.B. Beisenkhanov, S.K. Zharikov, I.K. Beisembetov, B. K. Kenzhaliev, T.K. Akhmetov, B Zh Seitov, *Phys. Solid State* 56 (11) (2014) 2307–2321.
[19] Cowern NEB, A. Cacciato, J.S. Custer, F.W. Saris, Wilfried Vandervorst, *Appl. Phys. Lett*. 68 (8) (1996) 1150–1152.
[20] Wenbo Li, Ling Li, Fangfang Wang, Liu Zheng, Jinghua Xia, Fuwen Qin, Xiaolin Wang, Yongping Li, Rui Liu, Dejun Wang, et al., *Chin. Phys. B* 26 (3) (2017), 037104.
[21] Dai Okamoto, Hiroshi Yano, Kenji Hirata, Tomoaki Hatayama, Takashi Fuyuki, *IEEE Electron. Device Lett*. 31 (7) (2010) 710–712.
[22] Dai Okamoto, Hiroshi Yano, Tomoaki Hatayama, Takashi Fuyuki, in: *Materials Science Forum*, vol. 645, Trans Tech Publ, 2010, pp. 495–498.
[23] G. Alfieri, T. Kimoto, J. *Appl. Phys*. 112 (6) (2012), 063717.
[24] P.O.Å. Persson, Lars Hultman, H. Jacobson, J.P. Bergman, Erik Janzén, J. M. Molina-Aldareguia, W.J. Clegg, T. Tuomi, *Appl. Phys. Lett*. 80 (25) (2002) 4852–4854.
[25] P.O.A. Persson, H. Jacobson, J.M. Molina-Aldareguia, J.P. Bergman, T. Tuomi, W. J. Clegg, Erik Janzén, Lars Hultman, in: *Materials Science Forum,* vol. 389, Trans Tech Publications Ltd., Zurich-Uetikon, Switzerland, 2002, pp. 423–426.
[26] Aoi Okada, Johji Nishio, Ryosuke Iijima, Chiharu Ota, Akihiro Goryu, Masaki Miyazato, Mina Ryo, Takashi Shinohe, Masaaki Miyajima, Tomohisa Kato, et al., *Jpn. J. Appl. Phys*. 57 (6) (2018), 061301.

[27] Shohei Hayashi, Tamotsu Yamashita, Junji Senzaki, Masaki Miyazato, Mina Ryo, Masaaki Miyajima, Tomohisa Kato, Yoshiyuki Yonezawa, Kazutoshi Kojima, Hajime Okumura, *Jpn. J. Appl. Phys*. 57 (4S) (2018), 04FR07.
[28] A. Gali, T. Hornos, N.T. Son, Erik Janzén, W.J. Choyke, *Phys. Rev. B* 75 (4) (2007), 045211.
[29] Hideharu Matsuura, Koichi Aso, Sou Kagamihara, Hirofumi Iwata, Takuya Ishida, Kazuhiro Nishikawa, *Appl. Phys. Lett.* 83 (24) (2003) 4981–4983.
[30] Dai Okamoto, Hiroshi Yano, Tomoaki Hatayama, Takashi Fuyuki, *Appl. Phys. Lett*. 96 (20) (2010), 203508.
[31] Hans Heissenstein, Christian Peppermueller, Helbig Reinhard, *J. Appl. Phys*. 83 (12) (1998) 7542–7546.
[32] T. Hornos, Gali Adam, Nguyen Tien Son, Erik Janzén, in: *Materials Science Forum,* vol. 556, Trans Tech Publ, 2007, pp. 445–448.
[33] Koutarou Kawahara, Michael Krieger, Jun Suda, Tsunenobu Kimoto, *J. Appl. Phys.* 108 (2) (2010), 023706.
[34] Souvick Mitra, Mulpuri V. Rao, N. Papanicolaou, K.A. Jones, M. Derenge, O. W. Holland, R.D. Vispute, S.R. Wilson*, J. Appl. Phys*. 95 (1) (2004) 69–75.
[35] Nobuo Tajima, Tomoaki Kaneko, Takahiro Yamasaki, Jun Nara, Tatsuo Schimizu, Koichi Kato, Takahisa Ohno, *Jpn. J. Appl. Phys*. 57 (4S) (2018), 04FR09.
[36] Atsuo Fukumoto, *Phys. Rev. B* 53 (8) (1996) 4458.
[37] Kuznetsov NI, A.S. Zubrilov, *Mater. Sci. Eng*., B 29 (1–3) (1995) 181–184.
[38] Koutarou Kawahara, Giovanni Alfieri, Tsunenobu Kimoto, *J. Appl. Phys.* 106 (1) (2009), 013719.
[39] Jochen Heyd, Gustavo E. Scuseria, Matthias Ernzerhof, *J. Chem. Phys*. 118 (18) (2003) 8207–8215.
[40] Georg Kresse, Jürgen Furthmüller, *Phys. Rev. B* 54 (16) (1996) 11169.
[41] Peter E. Bl€ochl, Projector augmented-wave method, *Phys. Rev. B* 50 (24) (1994) 17953.
[42] John P. Perdew, Kieron Burke, Matthias Ernzerhof, *Phys. Rev. Lett.* 77 (1996) 3865–3868.
[43] Michael E Levinshtein, Sergey L Rumyantsev, and Michael S Shur. John Wiley & Sons, 2001.
[44] Emmanuel Igumbor, Helga T. Danga, Ezekiel Omotoso, Walter Ernst Meyer, *Nucl. Instrum. Methods Phys. Res. Sect. B Beam Interact. Mater. Atoms* 442 (2019) 41–46.
[45] Emmanuel Igumbor, Okikiola Olaniyan, Refilwe Edwin Mapasha, Helga T. Danga, Ezekiel Omotoso, Walter Ernst Meyer, *Mater. Sci. Semicond. Process*. 89 (2019) 77–84.
[46] L. Gordon, Janotti Anderson, Chris G. Van de Walle, *Phys. Rev. B* 92 (4) (2015), 045208.

[47] Takuma Kobayashi, Kou Harada, Yu Kumagai, Fumiyasu Oba, Yu-ichiro Matsushita, Native point defects and carbon clusters in 4h-sic: a hybrid functional study, *J. Appl. Phys*. 125 (12) (2019), 125701.
[48] Chenguang Liu, Yuehu Wang, Yutian Wang, Zhiqiang Cheng, First-principles investigation of point defects at 4h-sic/sio 2 interface, in: *2018 1st Workshop on Wide Bandgap Power Devices and Applications in Asia (WiPDA Asia*), IEEE, 2018, pp. 135–139.
[49] Janusz Wozny, Andrii Kovalchuk, Zbigniew Lisik, Jacek Podgorski, Piotr Bugalski, Andrzej Kubiak, Lukasz Ruta, Dft simulation of stacking faults defects in 4h-sic, in: *2018 XIV-Th International Conference on Perspective Technologies and Methods in MEMS Design (MEMSTECH)*, vols. 65–68, IEEE, 2018.
[50] Blair R. Tuttle, Dangling bond defects in sic: an ab initio study, *Phys. Rev. B* 97 (4) (2018), 045203.
[51] Christoph Freysoldt, Jörg Neugebauer, G. Chris, Van de Walle, *Phys. Status Solidi* 248 (5) (2011) 1067–1076.
[52] Emmanuel Igumbor, Okikiola Olaniyan, Refilwe Edwin Mapasha, Helga T. Danga, Ezekiel Omotoso, Walter Ernst Meyer, *J. Phys. Condens. Matter* 30 (18) (2018), 185702.
[53] Emmanuel Igumbor, Refilwe Edwin Mapasha, Walter Ernst Meyer, J. *Electron. Mater*. 46 (7) (2017) 3880–3887.
[54] E. Igumbor, W.E. Meyer, *Mater. Sci. Semicond. Process*. 43 (2016) 129–133.
[55] T. Hornos, Gali Adam, Robert P. Devaty, Wolfgang J. Choyke, in: *In Materials Science Forum*, vol. 527, Trans Tech Publ, 2006, pp. 605–608.